Access to Generalized Parton Distributions at COMPASS

Wolf-Dieter Nowak for the COMPASS collaboration

University of Freiburg, Germany

Abstract. A brief experimentalist's introduction to Generalized Parton Distributions (GPDs) is given. Recent COMPASS results are shown on transverse target-spin asymmetries in hard exclusive ρ^0 production and their interpretation in terms of a phenomenological model as indication for chiral-odd, transverse GPDs is discussed. For deeply virtual Compton scattering, it is briefly outlined how to access GPDs and projections are shown for future COMPASS measurements.
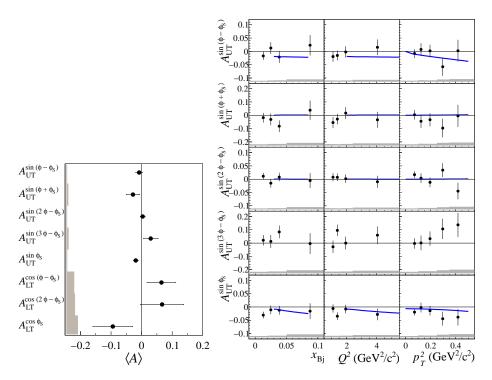
INTRODUCTION

The spin structure of the nucleon can be studied by singly or doubly polarized lepton-nucleon scattering, in particular through Deeply Virtual Compton Scattering (DVCS) and hard exclusive meson production (HEMP). For DVCS and for HEMP by longitudinal virtual photons, the process amplitude factorizes into a hard-scattering part and a soft part. The hard part, which describes the interaction of the virtual photon emitted by the incoming electron or muon with a quark from the nucleon, is exactly calculable in perturbative Quantum Chromodynamics (pQCD). The soft part contains information on the structure of the nucleon, which is encoded in Generalized Parton Distributions (GPDs) [1, 2, 3]. In the case of HEMP, it additionally contains the meson distribution amplitude that describes the structure of the meson. At leading twist and for a spin 1/2 target, there exist four chiral-even GPDs (H^f, $\widetilde{H}^f$, E^f, $\widetilde{E}^f$). The first two of them describe processes that conserve nucleon helicity and the last two those that involve nucleon helicity flip. The GPDs H^f and E^f are of special interest as they are related to the total angular momentum carried by the partons in the nucleon [4]. When Fourier-transformed to impact parameter space and for the case of vanishing longitudinal momentum transfer, GPDs provide a three-dimensional description of the nucleon in a mixed momentum-coordinate space, which is also known as 'nucleon tomography' [5, 6].

Different final states are sensitive to different (combinations of) GPDs. While DVCS is sensitive to all four of them, hard exclusive vector and pseudoscalar meson production are sensitive to only H^f, E^f and $\widetilde{H}^f$, $\widetilde{E}^f$, respectively. Here, f denotes a quark of a given flavor or a gluon. There exist also chiral-odd – often called transverse – GPDs, from which in particular H_T^f and $\bar{E}_T^f = 2\widetilde{H}_T^f + E_T^f$ are required [7, 8] for the description of exclusive π^+ electroproduction on a transversely polarised proton target [9]. It was recently shown [10] that the COMPASS data on exclusive ρ^0 production presented in this contribution are also sensitive to these GPDs. Unlike the case of HEMP by longitudinal virtual photons, there exists no proof of collinear factorization in the case of HEMP by transverse ones, which prevents an exact treatment as in the longitudinal case. In the phenomenological pQCD-inspired "GK" model [11, 12, 13], both cases are treated simultaneously by applying $k_\perp$ factorization instead, where $k_\perp$ represents parton transverse momentum, such that cross sections and spin-density matrix elements are well described in both cases. Using the GK parameterization of chiral-even GPDs [13], which is consistent with the HEMP data of HERMES [14] and COMPASS [15], recently almost all existing DVCS data were successfully described [16], thereby demonstrating consistency of the contemporary phenomenological GPD-based description of both DVCS and HEMP.

COMPASS RESULTS ON ρ^0 TRANSVERSE TARGET-SPIN ASYMMETRIES

In exclusive ρ^0 muoproduction on a transversely polarised target, $\mu N \to \mu' \rho^0 N'$, the cross section [17] contains eight azimuthal modulations sensitive to the transverse target polarisation, if – a very good approximation at COMPASS kinematics – the sensitivity to the polar angle of the virtual photon is neglected. These eight distinct azimuthal dependences give rise to five single-spin and three double-spin azimuthal asymmetries, which are described in more detail in Ref. [18]. The azimuthal angle between the lepton scattering plane and the production plane spanned by virtual photon and produced meson is denoted by ϕ and the one of the target spin vector about the virtual-photon

FIGURE 1. Left: Mean values $\langle A \rangle$ and uncertainties for all eight modulations [18]. The error bars (left bands) represent the statistical (systematic) uncertainties. Right: Five single-spin azimuthal asymmetries measured with unpolarized (U) beam and transversely (T) polarised target [18]. Error bars (bands) represent statistical (systematic) uncertainties. The curves show the predictions of the GPD model [10], in which $W = 8.1$ GeV/c^2 and $p_T^2 = 0.2$ (GeV/c)^2 for the left and middle panels, and at $W = 8.1$ GeV/c^2 and $Q^2 = 2.2$ (GeV/c)^2 for the right panels. and the asymmetry $A_{\mathrm{UT}}^{\sin(3\phi-\phi_S)}$ is assumed to be zero.

direction relative to the lepton scattering plane by ϕ_S. Unpolarised (longitudinally polarised) beam is denoted by U (L) and transverse target polarisation by T.

The mean values of all eight asymmetries are shown in the left panel of Fig. 1. The right panel shows the kinematic dependences of the five single-spin asymmetries on the Bjorken scaling variable x_{Bj}, on the photon virtuality Q^2, and on the square of p_T, which is the ρ^0 transverse momentum with respect to the virtual-photon direction. All details on the experimental set-up, event selection and background estimation are given in Ref. [18], as also on the extraction of asymmetries including subtraction of the semi-inclusive background using a two-dimensional binned maximum-likelihood fit and on the determination of the systematic uncertainty.

The already mentioned phenomenological GK model describes hard exclusive electroproduction of a light vector meson V at small x_{Bj} in the phenomenological 'handbag' approach, which also includes twist-3 meson wave functions. For a helicity amplitude $\mathscr{M}_{\mu\nu,\sigma\lambda}$, the subscripts specifying the helicities of the involved particles appear in the following order: vector meson (μ), final-state proton (ν), photon (σ), initial-state proton (λ). For brevity, the helicities $-1, -1/2, 0, 1/2, 1$ are labelled by only their signs or zero..

Results from calculations for the five single-spin and three double-spin asymmetries [10] are shown in the right panel of Fig. 1 as curves together with the data points. Of particular interest is the level of agreement between data and model calculations for the following four asymmetries that involve chiral-odd GPDs:

$$A_{\mathrm{UT}}^{\sin(\phi-\phi_s)} \propto -2\mathrm{Im}\left[\varepsilon\mathscr{M}_{0-,0+}^*\mathscr{M}_{0+,0+} + \mathscr{M}_{+-,++}^*\mathscr{M}_{++,++} + \frac{1}{2}\mathscr{M}_{0-,++}^*\mathscr{M}_{0+,++}\right], \tag{1}$$

$$A_{\mathrm{UT}}^{\sin(\phi_s)} \propto -\mathrm{Im}\left[\mathscr{M}_{0-,++}^*\mathscr{M}_{0+,0+} - \mathscr{M}_{0+,++}^*\mathscr{M}_{0-,0+}\right], \tag{2}$$

$$A_{\mathrm{UT}}^{\sin(2\phi-\phi_s)} \propto -\mathrm{Im}\left[\mathscr{M}_{0+,++}^*\mathscr{M}_{0-,0+}\right], \tag{3}$$

$$A_{\mathrm{LT}}^{\cos(\phi_s)} \propto -\mathrm{Re}\left[\mathscr{M}_{0-,++}^*\mathscr{M}_{0+,0+} - \mathscr{M}_{0+,++}^*\mathscr{M}_{0-,0+}\right]. \tag{4}$$

In Eq. 1, the virtual-photon polarisation parameter ε describes the ratio of longitudinal and transverse photon fluxes. Below, the subscripts ℓ and t denote the photon or meson helicities 0 and ± 1, respectively. The dominant $\gamma_\ell^* \to \rho_\ell^0$ transitions are described by helicity amplitudes $\mathscr{M}_{0+,0+}$ and $\mathscr{M}_{0-,0+}$, which are related to chiral-even GPDs H^f and E^f, respectively. These GPDs are used since several years to describe DVCS and HEMP data. The suppressed $\gamma_t^* \to \rho_t^0$ transitions are described by the helicity amplitudes $\mathscr{M}_{++,++}$ and $\mathscr{M}_{+-,++}$, which are likewise related to H^f and E^f. By the recent inclusion of transverse, i.e. chiral-odd GPDs, it became possible to also describe $\gamma_t^* \to \rho_\ell^0$ transitions. In their description appear the amplitudes $\mathscr{M}_{0-,++}$ related to chiral-odd GPDs H_T^f and $\mathscr{M}_{0+,++}$ related to chiral-odd GPDs $\bar{E}_T^f$, see Ref. [10] and references therein. The double-flip amplitude $\mathscr{M}_{0-,-+}$ is neglected. The transitions $\gamma_\ell^* \to \rho_t^0$ and $\gamma_t^* \to \rho_{-t}^0$ are known to be suppressed and hence neglected in the model calculations.

All measured asymmetries agree well with the calculations of Ref. [10]. In Eq. (1), the first two terms represent each a combination of chiral-even GPDs H^f and E^f. The inclusion of chiral-odd GPDs by the third term has negligible impact on the behaviour of $A_{\rm UT}^{\sin(\phi-\phi_S)}$, as can be seen when comparing calculations of Refs. [13] and [10]. The asymmetry $A_{\rm UT}^{\sin(\phi-\phi_S)}$ itself may still be of small magnitude, because for GPDs E^f in ρ^0 production the valence quark contribution is expected to be not large. This is interpreted as a cancellation due to different signs and comparable magnitudes of GPDs E^u and E^d [15]. Also, the small gluon and sea contributions evaluated in Ref. [13] cancel here to a large extent.

The asymmetries $A_{\rm UT}^{\sin\phi_S}$ and $A_{\rm LT}^{\cos\phi_S}$ represent imaginary and real part, respectively, of the same difference of two products $\mathscr{M}^*\mathscr{M}$ of two helicity amplitudes, where the first term of this difference represents a combination of GPDs H_T^f and H^f, and the second a combination of $\bar{E}_T^f$ and E^f. As can be seen in the left panel of Fig. 1, while no conclusion can be drawn on $A_{\rm LT}^{\cos\phi_S}$ because of larger experimental uncertainties, a non-vanishing value for $A_{\rm UT}^{\sin\phi_S}$ is measured. The asymmetry $A_{\rm UT}^{\sin(2\phi-\phi_S)}$ represents the same combination of GPDs $\bar{E}_T^f$ and E^f as the second term in $A_{\rm UT}^{\sin\phi_S}$. The observation of a vanishing value for $A_{\rm UT}^{\sin(2\phi-\phi_S)}$ implies that the non-vanishing value of $A_{\rm UT}^{\sin\phi_S}$ constitutes the first experimental evidence from hard exclusive ρ^0 leptoproduction for the existence of transverse GPDs H_T^f.

PROJECTIONS FOR FUTURE DVCS MEASUREMENTS AT COMPASS

The DVCS process, $\mu N \to \mu'\gamma N'$, is the theoretically cleanest process to experimentally access GPDs at COMPASS, as effects of next-to-leading order and subleading twist are under theoretical control [19]. The Bethe-Heitler (BH) process, i.e. real-photon radiation from the incoming or outgoing muon, has the same final state, so that the two process amplitudes interfere. The cross section for real-photon muoproduction hence contains an interference term I:

$$d\sigma \propto d\sigma^{BH} + (d\sigma_{unpol}^{DVCS} + P_\mu d\sigma_{pol}^{DVCS}) + e_\mu(\mathrm{Re}\, I + P_\mu \mathrm{Im}\, I). \tag{5}$$

Here, e_μ and P_μ denote charge and (longitudinal) polarization of the beam, respectively. As the CERN muon beam is derived from decaying beam pions, its 'natural' polarization changes sign upon beam charge reversal. In future COMPASS runs with an *unpolarized (U) proton target*, separate data sets will be taken with beam charge/polarization settings $+\leftarrow$ and $-\rightarrow$. They can be used to calculate either the *Beam Charge (C) and Spin (S) Difference*
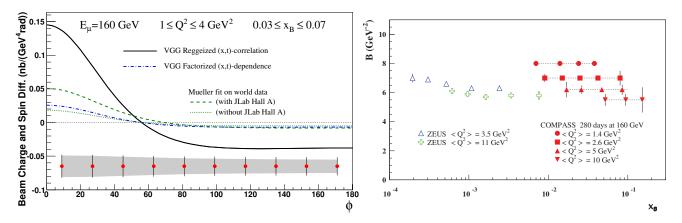
$$\mathscr{D}_{U,CS} \equiv d\sigma^{+\leftarrow} - d\sigma^{-\rightarrow} = 2(P_\mu d\sigma_{pol}^{DVCS} + e_\mu \mathrm{Re}\, I) \propto (c_0^I + c_1^I \cos\phi), \tag{6}$$

in which the pure BH contribution cancels, or the *Beam Charge and Spin Sum*

$$\mathscr{S}_{U,CS} \equiv d\sigma^{+\leftarrow} + d\sigma^{-\rightarrow} = 2(d\sigma^{BH} + d\sigma_{unpol}^{DVCS} + e_\mu P_\mu \mathrm{Im}\, I) \propto 2d\sigma^{BH} + c_0^{DVCS} + s_1^I \sin\phi, \tag{7}$$

in which the BH contribution does not cancel. For the last step in Eqs. 6 and 7, the DVCS amplitude was expanded [19] in $1/Q$ and only twist-2 terms are shown.

The analysis of the ϕ dependence of $\mathscr{D}_{U,CS}$ will provide via the term Re I the two leading-twist coefficients c_0^I and c_1^I. Both are for COMPASS kinematics related to the dominant real part of the Compton Form Factor (CFF) $\mathscr{H}$, which in leading order represents a weighted sum over flavors f, of convolutions of GPDs H^f with a kernel that describes the hard interaction between virtual photon and quark. Projections for a measurement of $\mathscr{D}_{U,CS}$ are shown for a given (Q^2, x_B) bin in the left panel of Fig. 2. Two of the curves were calculated using the 'VGG' GPD model [20] and visualize GPDs with high and with vanishing (x,t) correlations. The other two curves result from a fit [21] including NNLO corrections, which successfully describes DVCS data from the HERA collider, HERMES and JLab. The above

FIGURE 2. Projections for a future 2-year DVCS measurement at COMPASS with a luminosity of 1.2 fb^{-1} and 10% overall efficiency. Left: ϕ dependence of beam charge and spin difference $\mathscr{D}_{U,CS}$. Right: t slope parameter $B(x_B)$. For details see text.

mentioned recent calculation of Ref. [16] resembles the lowest curve. The analysis of the ϕ dependence of $\mathscr{S}_{U,CS}$ will provide via the term Im I the leading-twist coefficient s_1^I, the dominant contribution of which is related to the imaginary part of CFF $\mathscr{H}$.

In an alternative analysis ansatz, integration over ϕ removes the complete interference term and the ϕ-dependent DVCS contribution. This requires, for a given bin in Bjorken-x, to subtract the calculable BH contribution that is known to dominate at the lowest accessible x, from where its impact can be extrapolated. Isolating in this way the leading-twist quantity c_0^{DVCS}, its t dependence yields that of the DVCS cross section, $\frac{d\sigma}{dt}(x) \propto \exp{-B(x)t}$. In the simple ansatz $B(x) = B_0 + 2\alpha' \log\frac{x_0}{x}$, the shrinkage parameter α' is known since decades to describe the decrease in transverse nucleon size with increasing x. In the right panel of Fig. 2, the projected experimental uncertainties are shown for the Bjorken-x dependence of the slope parameter B. In a chiral-dynamics approach [22], the 'pion cloud' of the nucleon generates an increasing gluon density when x decreases below 0.15, which is the COMPASS kinematic region, and hence a significant increase in transverse nucleon size.

REFERENCES

1. D. Mueller *et al.*, Fortsch. Phys. **42** (1994) 101 [hep-ph/9812448].
2. A. V. Radyushkin, Phys. Lett. B **380** (1996) 417 [hep-ph/9604317].
3. X. -D. Ji, Phys. Rev. D **55** (1997) 7114 [hep-ph/9609381].
4. X. D. Ji, Phys. Rev. Lett. **78** (1997) 610 [hep-ph/9603249].
5. M. Burkardt, Phys. Rev. D **62** (2000) 071503 [Erratum-ibid. D **66** (2002) 119903] [hep-ph/0005108].
6. M. Burkardt, Int. J. Mod. Phys. A **18** (2003) 173 [hep-ph/0207047].
7. S. V. Goloskokov and P. Kroll, Eur. Phys. J. C **65** (2010) 137 [arXiv:0906.0460 [hep-ph]].
8. S. V. Goloskokov and P. Kroll, Eur. Phys. J. A **47** (2011) 112 [arXiv:1106.4897 [hep-ph]].
9. A. Airapetian *et al.* [HERMES coll.], Phys. Lett. B **682** (2010) 345 [arXiv:0907.2596 [hep-ex]].
10. S. V. Goloskokov and P. Kroll, Eur. Phys. J. C **74** (2014) 2725 [arXiv:1310.1472 [hep-ph]].
11. S. V. Goloskokov and P. Kroll, Eur. Phys. J. C **42** (2005) 281 [hep-ph/0501242].
12. S. V. Goloskokov and P. Kroll, Eur. Phys. J. C **53** (2008) 367 [arXiv:0708.3569 [hep-ph]].
13. S. V. Goloskokov and P. Kroll, Eur. Phys. J. C **59** (2009) 809 [arXiv:0809.4126 [hep-ph]].
14. A. Airapetian *et al.* [HERMES Collaboration], Phys. Lett. B **679** (2009) 100 [arXiv:0906.5160 [hep-ex]].
15. C. Adolph *et al.* [COMPASS coll.], Nucl. Phys. B **865** (2012) 1 [arXiv:1207.4301 [hep-ex]].
16. P. Kroll, H. Moutarde and F. Sabatie, Eur. Phys. J. C **73** (2013) 2278 [arXiv:1210.6975 [hep-ph]].
17. M. Diehl and S. Sapeta, Eur. Phys. J. C **41** (2005) 515 [hep-ph/0503023].
18. C. Adolph *et al.* [COMPASS coll.], Phys. Lett. B **731** (2014) 19 [arXiv:1310.1454 [hep-ex]].
19. A. V. Belitsky, D. Mueller and A. Kirchner, Nucl. Phys. B **629** (2002) 323 [hep-ph/0112108].
20. M. Vanderhaeghen, P. A. M. Guichon and M. Guidal, Phys. Rev. Lett. **80** (1998) 5064.
21. K. Kumerièki and D. Mueller, Nucl. Phys. B **841** (2010) 1 [arXiv:0904.0458 [hep-ph]].
22. M. Strikman and C. Weiss, Phys. Rev. D **69** (2004) 054012 [hep-ph/0308191].